

The lower hybrid frequency range wave emission in the ohmic discharge of the FT-2 tokamak

© V.V. Dyachenko, A.B. Altukhov, A.D. Gurchenko, E.Z. Gusakov, L.A. Esipov, A.N. Konovalov, S.I. Lashkul, A.Yu. Popov

Ioffe Institute,
St. Petersburg, Russia
e-mail: v.dyachenko@mail.ioffe.ru

Received December 27, 2022

Revised February 28, 2023

Accepted March 16, 2023

The paper presents observations of plasma intermediate frequency range wave emission ((200–1000) MHz) performed in ohmic discharge of the FT-2 tokamak. The dependencies of the RF signal amplitude and spectrum on the plasma parameters and on the location of the probes are presented. Two possible explanations for this effect is proposed. One of them is related to the distortion of the electron distribution function due to the strong ripple of the magnetic field in the FT-2 tokamak. Second one is related to the existence of a beam of run-away electrons, the buildup of a fan instability responsible for the generation of synchrotron radiation in the range (10–80) GHz, and a complex chain of nonlinear decay instabilities leading to such a strong decrease in the frequency of the observed oscillations.

Keywords: tokamak, lower hybrid current drive, high frequency oscillations, parametric decay instabilities.

DOI: 10.21883/TP.2023.05.56064.291-22

Introduction

The mechanism of transition from the induction-free current generation mode to the ion acceleration mode with the introduction of microwave power of the lower hybrid (NG) frequency range was studied for a number of years in FT-2 tokamak [1–3]. It was shown that this transition is more sharp than the theory predicts when the density exceeds a certain threshold value. For the FT-2 tokamak $\langle n_e \rangle_{thres} = 2.5 \cdot 10^{19} \text{ m}^{-3}$ in hydrogen plasma. The transition is accompanied by the intense oscillations at frequencies shifted relative to the frequency of the pumping wave by harmonics of the ion-cyclotron (IC) frequency (about 30 MHz in hydrogen plasma). These oscillations are observed at the plasma periphery using RF probes [4,5] and are associated with the excitation of parametric decay instability in the form of ion-cyclotron quasimodes [4]. It is the excitation of this instability in [6,7] that is attributed to the termination of generation of the induction-free current. This mechanism leads to a broadening of the oscillation spectrum of the pump wave towards low frequencies by a width of several IC frequencies. The oscillations should appear at the corresponding frequencies of the IC harmonics in the low frequency region. But all of the above applies to modes with current generation when HF power is introduced into the discharge. This paper describes intense radio frequency oscillations detected in the intermediate frequency range (100–1000) MHz in a purely ohmic discharge in the absence of HF power. Similar radiation, but in the range (0.6–1.5) GHz, was observed in modes with low density and runaway electrons in a tokamak FTU (Frascati) [8,9].

Section 1 contains a description of the experiment, the results are presented in section 2, the work is discussed in section 3.

1. Experiment description

Description of the experiment The interaction of NG waves with plasma was experimentally studied on a small research tokamak FT-2 ($R = 0.55 \text{ m}$, $a = 0.08 \text{ m}$, $B_T \leq 3 \text{ T}$, $I_p = 19\text{--}40 \text{ kA}$, $f_o = 920 \text{ MHz}$, $P_{RF} < 200 \text{ kW}$) and described in detail in [10]. The tokamak has a wide range of diagnostics tools: Thomson scattering for measuring the magnitude and profiles of electron temperature and density, a multi-chord microwave interferometer, a five-channel analyzer of charge atom fluxes, streaming diagnostics of hard (HXR) and soft (SXR) X-rays, optical spectroscopy, bolometric measurements, etc. Using an X-ray spectrometer registering quanta HXR with the energy $E_{hv} > 0.2 \text{ MeV}$ and synchrotron radiation receivers, the parameters of superheat escaping electrons were determined. The plasma current and the main discharge parameters in the described experiment varied within $I_p \approx (18\text{--}32) \text{ kA}$, $\langle n_e \rangle$ (the average density along the central chord) = $(0.5\text{--}5.0) \cdot 10^{19} \text{ m}^{-3}$, $T_e(0) = (350\text{--}400) \text{ eV}$, $T_i(0) = (80\text{--}100) \text{ eV}$, $B_T = (1.8\text{--}2.5) \text{ T}$.

Oscillations in a purely ohmic tokamak discharge in the frequency range (0–1100) MHz were studied in this paper. The oscillations were recorded using RF probes, their mutual arrangement is shown in Fig. 1. A single-pin RF probe P2 was placed on the side of the strong field (poloidal angle $\theta = 220^\circ$, the probe on the diaphragm

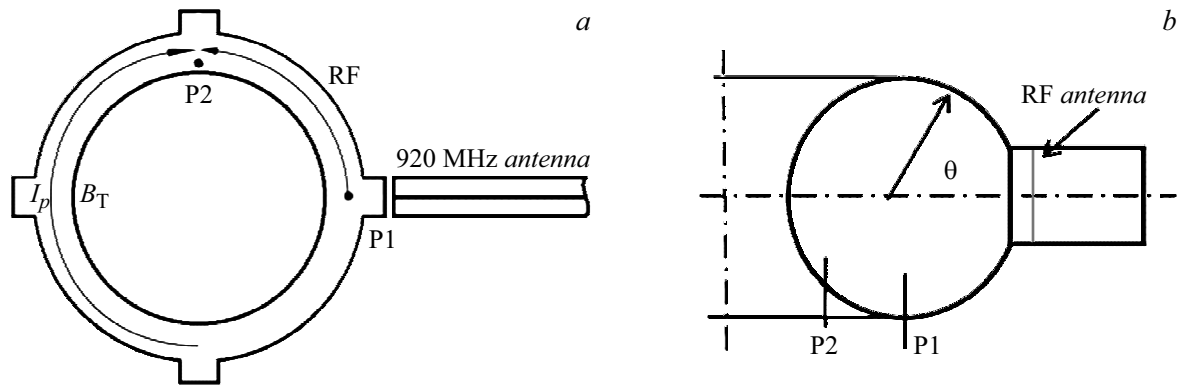


Figure 1. Arrangement of RF probes: *a* — view of the tokamak from above. The arrows show the direction of the current in the discharge and the predominant direction of wave propagation; *b* — the cross section of the tokamak. P1, P2 — RF probes.

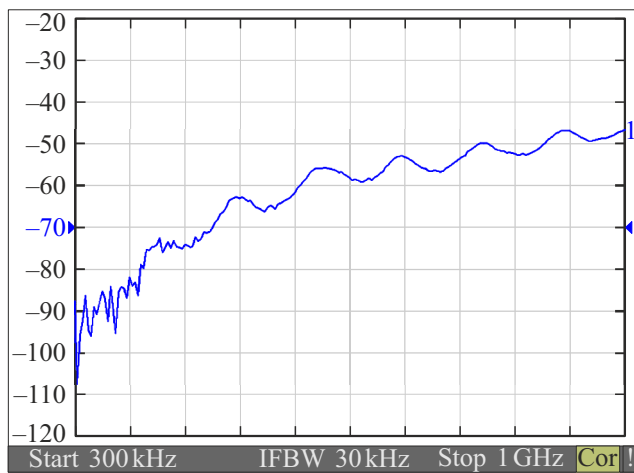


Figure 2. Frequency response of the RF probe. On the abscissa axis — frequency from 300 kHz to 1 GHz, division price — 100 MHz; on the ordinate axis — sensitivity of the probe in logarithmic scale.

slice, $r = 8$ cm). The same RF probe P1 is installed in the antenna section ($\theta = 270^\circ$, in the shadow of the diaphragm, $r = 8.5$ cm). The RF signal from the probes was fed through decoupling transformers to the spectrum analyzers. The probes P1 and P2 are structurally the same, and the signal transmitting circuits are also the same. Most of the measurements were performed using a broadband (up to 8 GHz) digital four-channel oscilloscope Keysight MSOS804A. In our case, the oscilloscope analyzed the radiation signal in the frequency band from zero to 1.1 GHz for time intervals (0.1–3.0) ms. The presence of spectral components, their temporal evolution and intensity were determined during processing and analysis of the data obtained. Due to the small size of the probes ($l = 5$ mm), their sensitivity is very low (from -80 to -40 dB in the frequency band (0–1) GHz, but the amplitude-frequency response (frequency response) of the probes is quite smooth with a smooth decrease in sensitivity to the low frequency region. The frequency response of the probes was studied

using the Agilent E5061B circuit analyzer on a broadband test bench of — coaxial section. Fig. 2 shows the frequency response of such a probe. The oscillations observed in the plasma have the ability to be re-emitted into the tokamak chamber and are well recorded as radiation using LH antenna waveguides used as a receiving antenna with frequencies above 700 MHz (waveguide cutoff frequency). The main material of the publication is based on data obtained from RF probes P1,2.

2. Experimental results

The described results were obtained during experiments on maintaining current using LH waves, but in the ohmic phase of the discharge before applying RF power in the quasi-stationary phase of the discharge. During the application of RF power at $\langle n_e \rangle 3 \cdot 10^{19} \text{ m}^{-3}$, there was a „decoupling“ of the bypass voltage, indicating a partial replacement of the ohmic current with the current induced by the pump wave (Fig. 3).

The probe signal began to be recorded in 1 ms before the start of the RF pulse and (1–2) ms during the pulse. This made it possible to obtain spectra in one discharge for the purely ohmic stage of the discharge and together with the RF power. When studying the oscillation of parametric decay instabilities at densities close to the threshold of termination of current generation, the existence of intense bursts of oscillations was found even in the ohmic stage of the tokamak discharge. Flashes lasting several tens of microseconds had a repetition rate of several kHz for different plasma densities, their number and amplitude decreased with increasing discharge density (Fig. 4, *a*).

Frequency analysis of the flashes carried out in the frequency range from 0 to 1000 MHz showed that this radiation is a packet of several (3–6) frequency peaks linked together, the amplitude of which exceeds the noise level by 10–30 dB. The packet width is 100–300 MHz in different discharge modes. An example of such a spectrum is shown in Fig. 5, probe P2. There are practically no such frequency packets between flashes. The spectrum

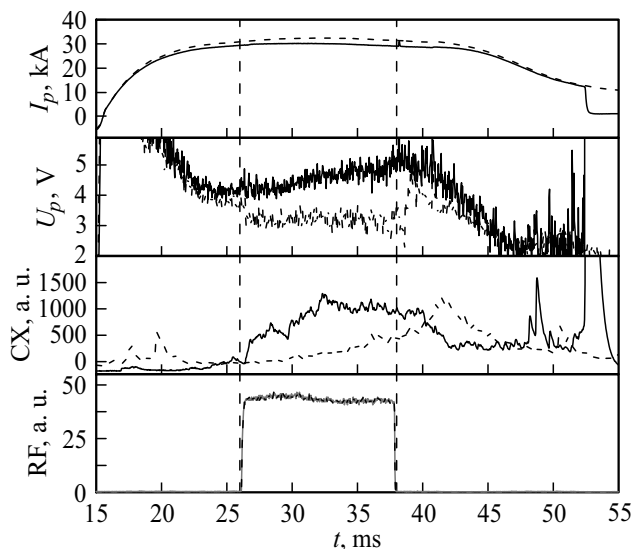


Figure 3. Evolution of the main discharge parameters in ohmic mode (solid line) and with the introduction of RF power (dash). I_p — plasma current, U_p — bypass voltage, CX — recharge atom flux with energy 980 eV, RF — RF pulse.

analysis was conducted in the „window“ with a duration of 1 ms. The spectrum was averaged to a standard technique, namely, the signal was divided into 100 time intervals, for each of which the spectral power density was calculated, after which the obtained spectra were added point-by-point and normalized by the number of time intervals.

The behavior of such a packet depending on the discharge density is of the highest interest. The packet occupies the frequency range from 350 MHz with the lowest discharge density $\langle n_e \rangle = (0.5-0.7) \cdot 10^{19} \text{ m}^{-3}$ and, in fact, is not limited by high frequencies. The boundaries of the packet are well formed with the higher density, and it shifts towards higher frequencies — up to 800 MHz with an increase in the density of the hydrogen plasma to $3.5 \cdot 10^{19} \text{ m}^{-3}$. The amplitude and the number of peaks in the spectrum decrease rapidly to the noise level with a further increase of the density in the ohmic discharge. The main pronounced peaks in the packet are separated from each other by 30–35 MHz in hydrogen plasma, regardless of density, this frequency value lies in the region of ion-cyclotron frequencies for the operating value of the toroidal field (2.2 T on the toroidal axis). The behavior of the packet (probe P2) is illustrated in Fig. 6 for different values of the discharge concentration. The probe P1 records the same signal in nature, but its amplitude significantly depends on the depth of immersion of the probe.

The dependence on the magnitude of the toroidal magnetic field at the concentration of hydrogen plasma $\langle n_e \rangle \approx 1.7 \cdot 10^{19} \text{ m}^{-3}$ shows that there are practically no fluctuations with BT below 1.8 T, and the entire package is slightly shifted to higher frequencies when the magnetic field increases to 2.5 T. The dependence on the magnitude of the discharge current in the hydrogen plasma within

the statistical spread and measurement range has not been detected.

The qualitatively described picture is preserved in deuterium plasma, an example of a frequency packet is shown in Fig. 5, *b*, only „thin“ packet structure is complicated due to peaks shifted in frequencies by the value of the ion-cyclotron frequency of deuterium, approximately by 15–17 MHz. Only noise peaks at such shifted frequencies are visible in Fig. 5, *b*. But hydrogen is always present in deuterium plasma and apparently suppresses the rocking of deuterium resonances. In addition, cyclotron frequencies are multiples of each other and indistinguishable on the spectrum. Fig. 5 also shows that the packets in hydrogen and deuterium plasmas are shifted in frequencies by about 150 MHz with the same discharge parameters.

It is interesting to note that when an RF pulse with a power of 60–80 kW „is applied, the flash“ oscillation pattern detected during ohmic heating (Fig. 4, *a*) disappears, the signals from the probes have a continuous noise appearance with a significantly larger amplitude (Fig. 4, *b*). But RF power does not affect the existence and behavior of the packet as long as the plasma concen-

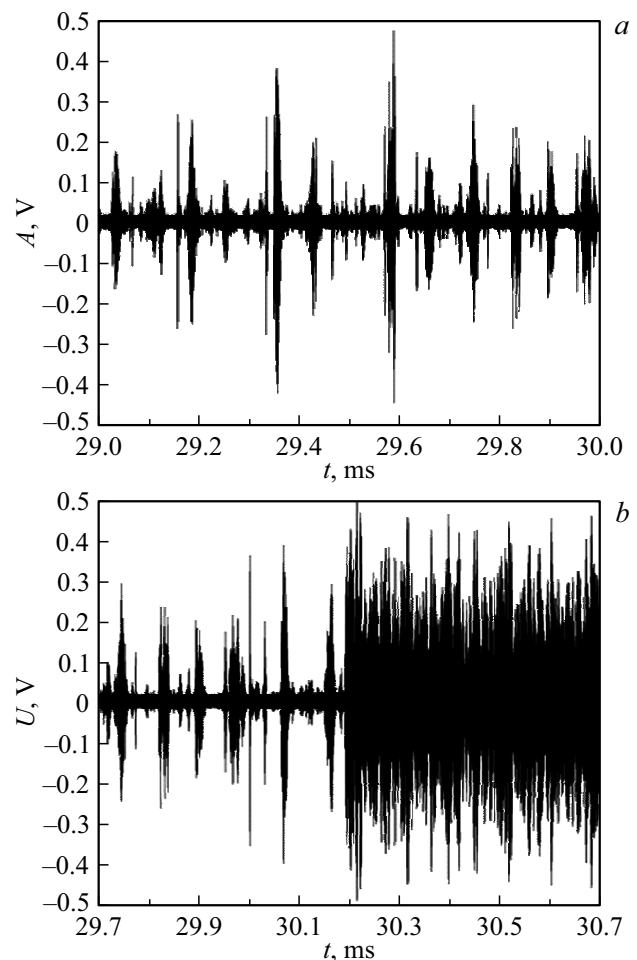


Figure 4. Type of plasma radiation: *a* — in the ohmic stage of discharge, probe P2; *b* — in the absence and presence (starting from $t = 30$ ms) of RF power, probe P2.

tration is below the threshold (at which current generation stops), $\langle n_e \rangle < 2.5 \cdot 10^{19} \text{ m}^{-3}$ (Fig. 7, *a-d*), but the packet width increases slightly towards high frequencies. But if in the ohmic phase of the discharge at a density of $\langle n_e \rangle < 3.5 \cdot 10^{19} \text{ m}^{-3}$ the oscillations almost disappeared, then the packet only was only enhanced under the impact of RF power with this density and moved close to the peak of the pump wave with $f_0 = 920 \text{ MHz}$, as shown by probe P2 (Fig. 7, *e, f*) at $\langle n_e \rangle > \langle n_e \rangle_{\text{thres}}$.

3. Results and discussion

It is known that a beam of escaping high-energy electrons is produced in tokamaks at the moment of discharge formation, which exist for a prolonged time with low discharge densities. These electrons are a source of synchrotron radiation at frequencies from 30 GHz and higher, they also contribute to the frequency spectra at the lowest density (Fig. 6, *a*) [9]. The oscillations described

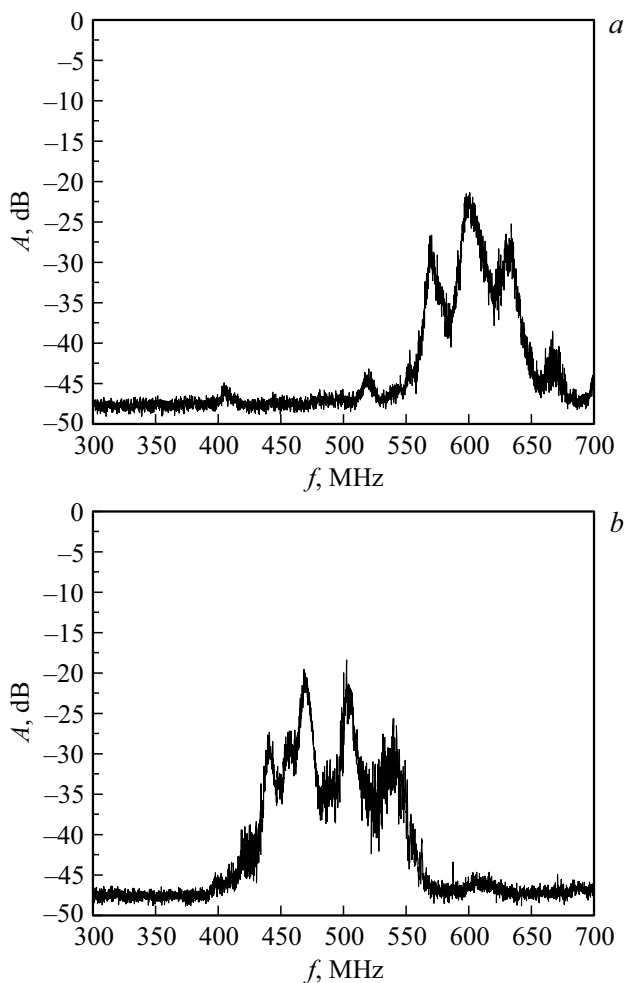


Figure 5. Example of the frequency spectrum of radiation during one of the flashes, $\langle n_e \rangle = 2.0 \cdot 10^{19} \text{ m}^{-3}$; *a* — in hydrogen plasma, *b* — in deuterium. Along the ordinate axis — the amplitude of the spectral components on a logarithmic scale.

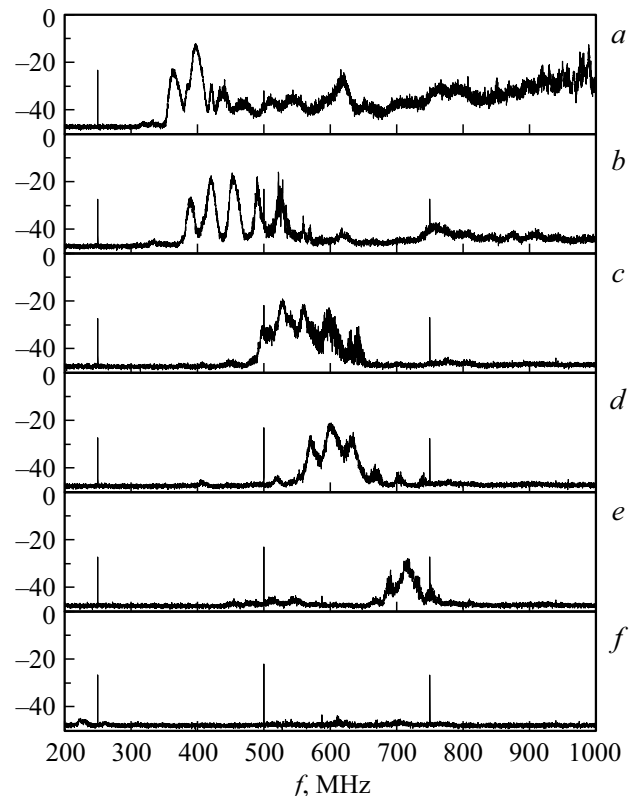


Figure 6. Spectral packet behavior depending on density $\langle n_e \rangle$: *a* — $0.5 \cdot 10^{19} \text{ m}^{-3}$, *b* — $1.2 \cdot 10^{19} \text{ m}^{-3}$, *c* — $1.5 \cdot 10^{19} \text{ m}^{-3}$, *d* — $2.0 \cdot 10^{19} \text{ m}^{-3}$, *e* — $2.5 \cdot 10^{19} \text{ m}^{-3}$, *f* — $3.5 \cdot 10^{19} \text{ m}^{-3}$; $B_{T0} = 2.2 \text{ T}$. Along the ordinate axis — the amplitude of the spectral components on a logarithmic scale.

here lie in the region of lower, so-called low-hybrid (LH) frequencies, $< 1 \text{ GHz}$.

The distribution of calculated LH frequency values for cold hydrogen (without impurities) plasma over the tokamak cross section for two density values and $B_{T0} = 2.2 \text{ T}$ is shown in Fig. 8. The width of the packet can be determined using Fig. 6 (for certainty at the level of -40 dB). Only the low-frequency boundary of the spectrum is sharply outlined with the lowest density (Fig. 6, *a*) (but the actual LH fluctuations, according to calculation, should not exceed 400 MHz according to Fig. 8), therefore, the packet width was artificially limited to 200 MHz. The measured width of the spectrum (region of existence) of radiation, depending on the density, is shown in Fig. 9. The radiation practically disappears (Fig. 6, *f*) with a density of $3.5 \cdot 10^{19} \text{ m}^{-3}$, so the chart is interrupted. Also, the boundary of the phenomenon from the very low density side has not been determined (measured) due to the instability of the plasma discharge. Then perhaps there is a region of optimal density values $\langle n_e \rangle \approx (1-2) \cdot 10^{19} \text{ m}^{-3}$ for the existence of observed oscillations proceeding from the signal intensity and frequency saturation. Using Fig. 8 it is possible to qualitatively distinguish the spatial region of the generation (existence) of radiation in the discharge cross section using

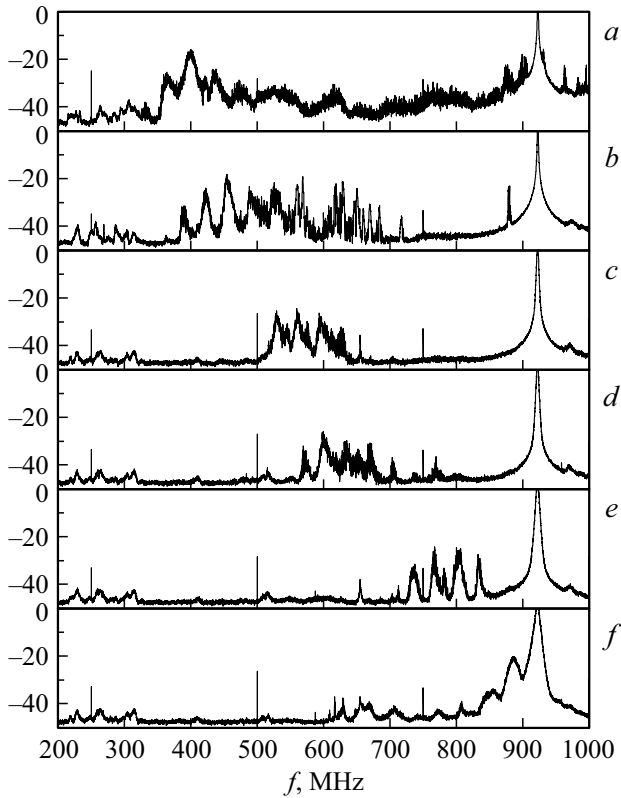


Figure 7. Spectral packet behavior depending on density $\langle n_e \rangle$ at $B_{T0} = 2.2$ T in the presence of RF power: *a* $0.5 \cdot 10^{19} \text{ m}^{-3}$, *b* $1.2 \cdot 10^{19} \text{ m}^{-3}$, *c* $1.5 \cdot 10^{19} \text{ m}^{-3}$, *d* $2.0 \cdot 10^{19} \text{ m}^{-3}$, *e* $2.5 \cdot 10^{19} \text{ m}^{-3}$, *f* $3.5 \cdot 10^{19} \text{ m}^{-3}$.

the example of the curve for density $\langle n_e \rangle = 1.2 \cdot 10^{19} \text{ m}^{-3}$. It can be seen that LH oscillations can be generated in two regions along the plasma cross section both at $R = R_0$ and at $R = R_0$. But preference should be given to the outer side of the torus at $R = 55\text{--}60$ cm ($R_0 = 55$ cm). This argument is supported by the fact that in this range of values R , the magnitude of the toroidal field varies from 2.2 to 2.0 T, respectively, the ion-cyclotron (IC) frequency for hydrogen plasma in this region is equal to 33–30 MHz. It is precisely this frequency shift that occurs between the peaks of the „fine“ structure of the spectral packet in Fig. 6. The estimation of the oscillation localization region for different density values is shown in Fig. 10. The generation region shifts deeper into the discharge $R < R_0$ with increasing density and the signal disappears. In general, vibrations (radiation) are formed in the central regions of the discharge. According to the observed frequency range, depending on the density and isotopic composition, the observed oscillations have all the signs of LH oscillations, but with modulation by IC frequencies.

The study of the spectral structure of RF probe signals presented above was performed with averaging over 100 consecutive samples, each with a duration of 0.1 ms. The spectra of probe signals were calculated with an improved time resolution for „windows“ with a duration of 0.2048 μs ,

taken sequentially with 10 averages for a more detailed study of their temporal dynamics. The reduction of the frequency resolution to the value of $\delta f \approx 2.44$ MHz, of course, was the price of such an approach which, nevertheless, is quite acceptable for analyzing the spectral features of the signals under consideration. An example of the time evolution of the signal power spectrum of the probe P2 is shown in Fig. 11, where a quasi-periodic structure is clearly visible in the range 550–850 MHz. The period of fluctuations in the probe signal power increases slightly in the considered time interval from 29 to 31 ms, taken in ohmic discharge, so that the change in the frequency of these flashes can be represented in terms of a slight linear frequency modulation: $f(t) = f_0 - b(t - t_0)$, where $f_0 = 4. \text{ kHz}$, $b = 0.17 \cdot 10^6 \text{ s}^{-2}$.

The structure of the oscillations shown in Fig. 11 is of particular interest. In particular, the time resolution used

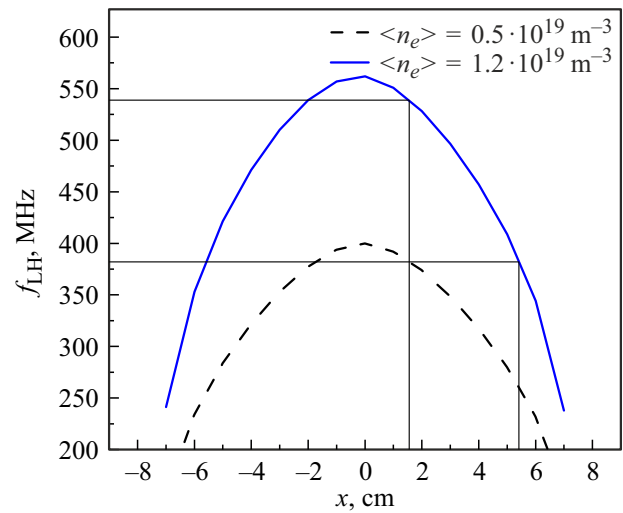


Figure 8. Example of LH frequency distribution over the tokamak cross section for two density values, $B_{T0} = 2$ T. In hydrogen.

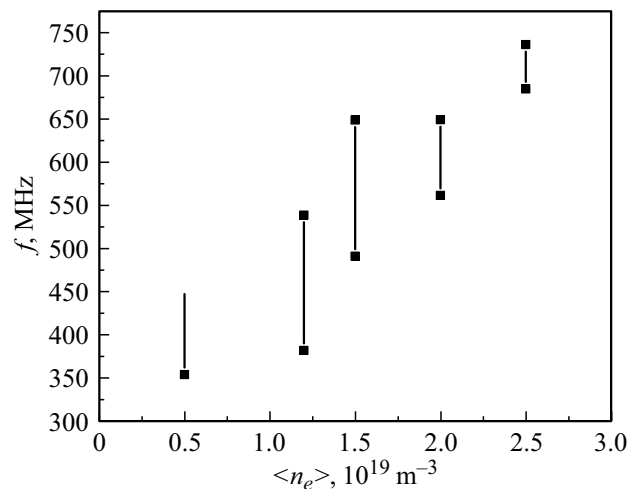


Figure 9. Dependence of the spectral width of the packet on the discharge density.

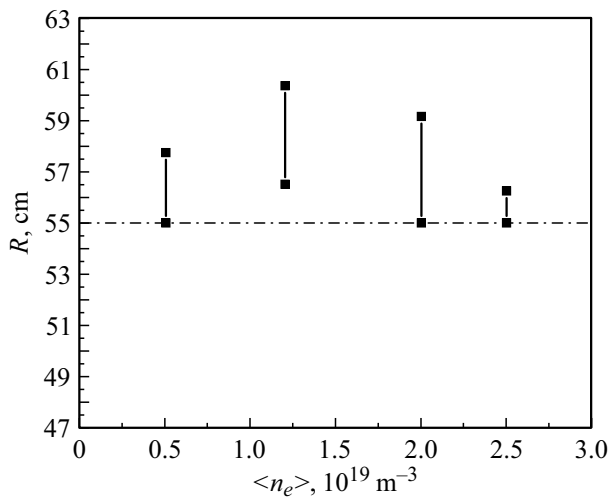


Figure 10. Evaluation of the localization of the radiation generation region depending on the discharge density.

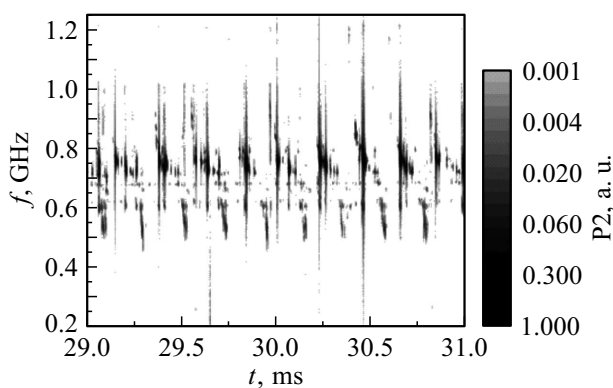


Figure 11. Evolution of the signal power spectrum of the probe P2 in the stationary part of the ohmic discharge with a duration of 2 ms.

was sufficient to demonstrate not only a frequency drop in the observed signal by the amount of $\Delta f \approx 40$ MHz for $80\text{--}100\ \mu\text{s}$, but also its flash character for their most intense high-frequency part near 800 MHz. Examples of such flashes are shown in Fig. 12 for two different time intervals, each with a duration of $100\ \mu\text{s}$. When calculating the signal spectrum with averaging at times greater than $100\ \mu\text{s}$, spectral flashes merge into a spectral maximum of a complex shape, often including separate spectral lines (see, for example, Fig. 6).

Signals on probes P1 and P2 located in different toroidal sections had spectral maxima at close frequencies, at the same time, their absolute value depended on the spatial position of the probe relative to the last closed magnetic surface. The power spectra of these signals calculated for time implementations with a duration of $0.2048\ \mu\text{s}$, taken sequentially with 9765 averages in the frequency range from 450–850 MHz are shown in Fig. 13. The most intense oscillations were observed on the signals of both probes in the 730–800 MHz range and the spectral

maximum was shifted by 30 MHz in a larger direction for the probe P2 installed from the side of a strong magnetic field, compared to the maximum on the spectrum for the probe P1, located on the weak field side. Lower intensity maxima were observed for the low-frequency part of the oscillations shown in Fig. 11, in the range of 530–610 MHz. In particular, 20 dB below the high-frequency maximum for probe P2, the difference was significantly less for probe P1 or 7–8 dB.

A detailed comparison of the two signals from different probes was made using correlation analysis by calculating the cross-correlation function for each spectral component of the signals with 9765 averages. Fig. 13, *b* shows the corresponding coherence spectrum, and Figure 13, *c* shows their cross-phase. A significant level of coherence, above 70%, was observed at the frequency of the spectral maximum of the probe signal P2 (767 MHz). A second burst of coherence was observed with a lower frequency in the spectral maximum region for the probe P1 (738 MHz), slightly above 30%. High levels of coherence were also observed from 12 to 16% in the low frequency region (540 and 600 MHz). The frequency dependence of the cross-phase signals (Fig. 13, *c*) had a linear dependence in regions with high coherence while its slope coefficient was the same for both ranges $\Delta\psi/\Delta f = 3.5 \pm 0.1$ deg/MHz. The presence of linear sections in the cross-phase is a clear indication of the presence of toroidal radiation propagation in the intermediate frequency range, and at the same

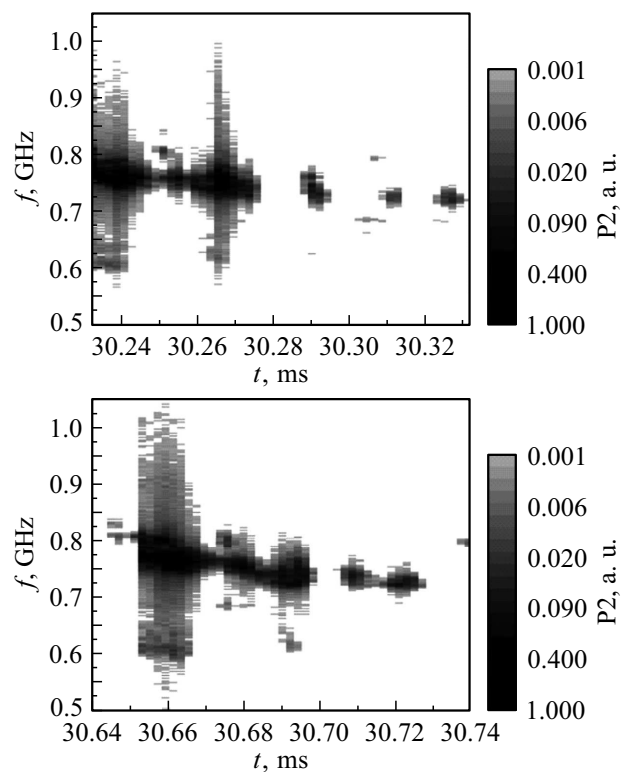


Figure 12. Spectra of the probe P2 signal for two different discharge intervals, demonstrating the evolution of the high-frequency part of the radiation oscillations.

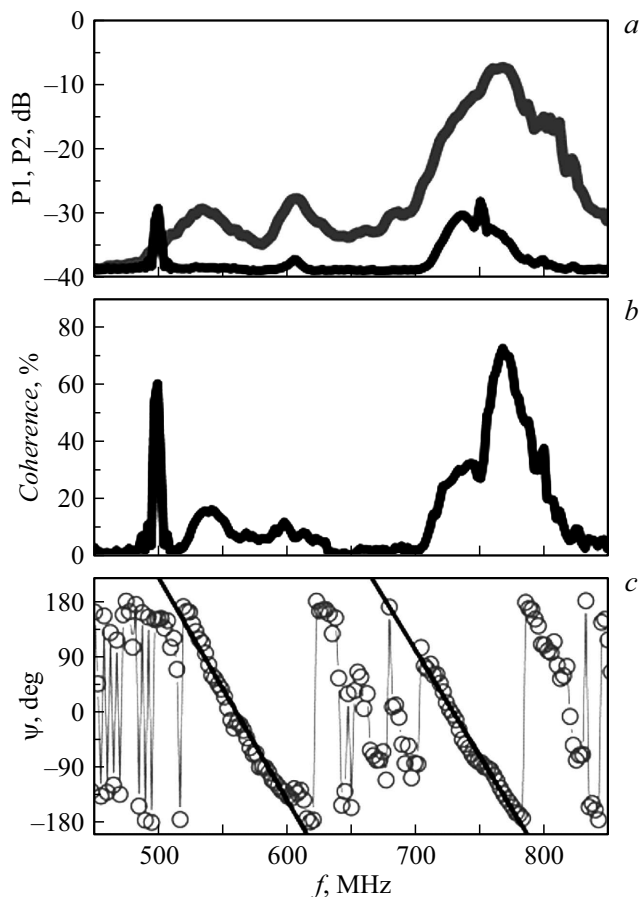


Figure 13. Results of correlation analysis of probe signals P1 and P2; *a* — power spectra of each signal, *b* — coherence, *c* — cross-phase (gray circles) and linear approximations of cross sections-phases (solid black lines).

speed for the high-frequency (710–820 MHz) and low-frequency (520–620 MHz) ranges. It should be noted that the presented result is well reproducible when the tokamak discharge is repeated, in particular, the shapes of the signal spectra and coherence are preserved, and the cross-phase slope coefficient, while remaining the same for high- and low-frequency regions, can reach up to $\Delta\psi/\Delta f = 3.9 \pm 0.1$ deg/MHz. Assuming that the radiation of the intermediate range propagates between the two probes along the shortest arc, it is possible to obtain an estimate for the corresponding velocity: $v = (c/3.3[-]c/2.9)$, where c — the speed of light.

One of the suggested mechanisms explaining the nature of this phenomenon may be related to the strong corrugation of the toroidal field and the toroidal drift of the ions trapped in, which causes a distortion of the ion distribution function [11] towards depletion of the high-energy part of the spectrum, which in turn, can lead to the rocking of ion Bernstein oscillations with LH frequencies. These oscillations near their LH resonance can transform first into slow, and then into oblique Langmuir waves capable of escaping from the plasma [11]. Such an assumption could

also explain the modulation of radiation by ion-cyclotron frequencies.

In conditions of powerful ion heating with the help of neutral beams or IC resonance, intense high-energy „tails“ are formed on the ion distribution function. They can generate so-called ion-cyclotron radiation, including at high harmonics of the ion-cyclotron frequency [12,13]. There are no such „tails“ in the ohmic, rather cold, discharge of the FT-2 tokamak. No noticeable radiation is observed in the ohmic discharge at the frequencies of regular ion-cyclotron harmonics in the low-frequency part of the observed spectrum (up to 100 MHz).

On the other hand, it is known that there is a beam of accelerated electrons in low-density modes in tokamaks that disappears with increasing density, and the associated powerful synchrotron radiation at frequencies above 10 GHz [12]. A beam of accelerated electrons causes the development of a fan instability [14], which has a „flash“ character. It is possible that this radiation can lead to the excitation of a chain of parametric decay instabilities that significantly lower the radiation frequencies [15]. The authors of [8,9] tend to such an explanation.

Both explanations need detailed theoretical studies.

Conclusions

Experiments on the FT-2 tokamak revealed intense oscillations in the form of flashes in the LH frequency range 0.2–1.0 GHz, modulated by IC harmonics, in ohmic modes with low plasma density. As the estimates show, the fluctuations originate from the central regions of the discharge. These oscillations have the ability to be re-emitted outwards and recorded by external antennas. Cross-correlation analysis of probe signals estimates the propagation velocity of oscillations in plasma to be three times less than the speed of light.

The smooth transition of the observed oscillations from the ohmic phase of the discharge to the heating phase may indicate the interaction of the pump wave with the fluctuations existing in the LH plasma and their subsequent amplification without involving the mechanism of parametric decay instability. This assumption is supported by very low thresholds of excitation of instability in RF power, measured in [4].

The nature of the observed radiation is still unclear.

Funding

FT-2 tokamak was operated and basic diagnostics was carried out with the support of the state contract FTI 0040-2019-0023. High-frequency measurements were performed with the support of the state contract FTI 0034-2021-0002, and their correlation analysis was supported by the state contract FTI 0034-2021-0001.

Conflict of interest

Translated by A.Akhtyamov

The authors declare that they have no conflict of interest.

References

- [1] V.N. Budnikov, V.V. Dyachenko, M.A. Irzak, E.R. Its, S.I. Lashkul, K.A. Podushnikova. A.Yu. Stepanov, O.N. Shcherbinin, M.J. Vildjunas. *Proc. of the 22st EPS Conf on Cont. Fus. and Pl. Phys.* (Bournemouth, 1995), p. IV, 385–387.
- [2] S.I. Lashkul, A.B. Altukhov, A.D. Gurchenko, E.Z. Gusakov, V.V. Dyachenko, L.A. Esipov, M.A. Irzak, M.Yu. Kantor, D.V. Kuprienko, A.N. Savelyev, A.Yu. Stepanov, S.V. Shatalin. *Fizika Plazmy*, **41** (12), 1069 (2015) (in Russian).
- [3] S.I. Lashkul, A.B. Altukhov, A.D. Gurchenko, E.Z. Gusakov, V.V. Dyachenko, L.A. Esipov, A.N. Konovalov, D.V. Kuprienko, S.V. Shatalin, A.Yu. Stepanov. *Fizika Plazmy*, **48** (5), 387 (2022) (in Russian). DOI: 10.31857/S0367292122200033
- [4] V.V. Dyachenko, A.N. Konovalov, A.Y. Stepanov, A.B. Altukhov, E.Z. Gusakov, L.A. Esipov, S.I. Lashkul, S.V. Shatalin. *Plasma Phys. Rep.*, **45** (12), 1134 (2019).
- [5] V.N. Budnikov, V.V. Dyachenko, L.A. Esipov, S.I. Lashkul, V.O. Aleksandrov, I.E. Saharov, S.V. Shatalin. *Proc. of the 19-th Conf. on Contr. Fusion and Plasma Physics* (Innsbruck, 1992), p. 11, 997–1000.
- [6] Y. Takase, M. Porkolab, J. Schuss, R. Watterson, C. Fiore. *Phys. Fluids*, **28**, 983 (1985).
- [7] R. Cesario, L. Amicucci, A. Cardinali, C. Castaldo, M. Marinucci, F. Napoli, F. Paoletti, D. De Arcangelis, M. Ferrari, A. Galli, G. Gallo, E. Pullara, G. Schettini, A.A. Tuccillo, *Nucl. Fusion*, **54**, 043002 (2014).
- [8] W. Bin, C. Castaldo, F. Napoli, P. Buratti, A. Cardinali, A. Selce, O. Tudisco (FTU Team). *Phys. Rev. Lett.*, **129**, 045002 (2022).
<https://doi.org/10.1103/PhysRevLett.129.045002>
- [9] P. Buratti, W. Bin, A. Cardinali, D. Carnevale, C. Castaldo, O. D’Arcangelo, F. Napoli, G.L. Ravera, A. Selce, L. Panaccione, A. Romano (FTU Team). *Plasma Phys. Control. Fusion*, **63**, 095007 (2021). DOI: 10.1088/1361-6587/ac138c
- [10] S.I. Lashkul, A.B. Altukhov, A.D. Gurchenko, E.Z. Gusakov, V.V. Dyachenko, L.A. Esipov, V.A. Ivanov, O.A. Kaledina, M.Yu. Kantor, A.N. Konovalov, D.V. Kuprienko, M.I. Mironov, S.V. Shatalin, A.V. Sidorov, A.Yu. Stepanov, F.V. Chernyshev, N.V. Tropin. *Fizika Plazmy*, **46** (9), 771 (2020) (in Russian).
- [11] A.A. Galeev, R.Z. Sagdeev. „*Neoklassicheskaya*“ *teoriya dif-fuzii*, in the book *Voprosy teorii plazmy* (Atomizdat, M., 1973), vol. 7, 11 (in Russian).
- [12] K.G. McClements, R. D’Inca, R.O. Dendy, L. Carbajal, S.C. Chapman, J.W.S. Cook, R.W. Harvey, W.W. Heidbrink, S.D. Pinches. *Nucl. Fusion*, **55**, 043013 (2015).
- [13] N.N. Gorelenkov. *New J. Phys.*, **18**, 105010 (2016).
- [14] S.I. Lashkul, V.V. Rozhdestvensky, A.B. Altukhov, V.V. Dyachenko, L.A. Esipov, M.Yu. Kantor, S.V. Krikunov, D.V. Kuprienko, A.Yu. Stepanov. *Tech. Phys. Lett.*, **38** (12), 1073 (2012).
- [15] V.V. Parail, O.P. Pogutse. *Uskorennye elektrony v tokamake*, in book *Voprosy teorii plazmy* (Energoizdat, M., 1982), vol. 11, p. 5–55 (in Russian).